More accurate than MRI measurement of tumor size in breast cancer by using the peri-tumoral halo uptake layer method of the ^{18}F-FDG PET/CT scan

Seol Hoon Park[1] MD,
Minjung Seo[1] MD,
Hye-Jeong Choi[2] MD, PhD,
Kyungkyg Bae[3] MD,
Minseo Bang[3] MD,
Sungmin Jun[4] MD, PhD

1. Department of Nuclear Medicine
2. Department of Pathology
3. Department of Radiology, Ulsan University Hospital, University of Ulsan College of Medicine, Ulsan, Korea
4. Department of Nuclear Medicine, Kosin University Gospel Hospital, Kosin University College of Medicine, Busan, Korea

Keywords: Breast cancer - Tumor size - Peritumoral halo layer - MRI - ^{18}F-FDG PET/CT

Corresponding author:
Sungmin Jun MD
Kosin University Gospel Hospital,
262, Gamcheon-ro,
Seo-gu, Busan, Republic of Korea, 49267
fanace@daum.net
Tel: 82-51-990-6384 / Fax: 82-51-990-3044

Received:
23 April 2018
Accepted revised:
26 June 2018

Abstract

Objectives: To evaluate the reliability of a method using the peri-tumoral halo layer (PHL) for assessing tumor size in breast cancer patients on the fluorine-18-fluorodeoxy glucose positron emission tomography/computed tomography (^{18}F-FDG PET/CT) scan compared to MRI and pathology. **Subjects and Methods:** Among 121 patients with breast cancer who underwent both ^{18}F-FDG PET/CT and MRI between March 2013 and June 2016, 59 patients were included in this study. Exclusion criteria were as follows: history of neoadjuvant therapy, history of pre-operative mammotome, insufficient pathologic/radiologic size report, clustered tumor, positive tumor resection margin, ^{18}F-FDG non-avid tumor. The PHL was examined by two nuclear medicine physicians. Tumor sizes (longest diameters) on ^{18}F-FDG PET/CT were estimated using margins defined as the inner line of the PHL. Pathologic tumor sizes were utilized as reference standards. **Results:** The PHL of each tumor was most commonly designated as the 20%-30% band of the maximum standardized uptake value (SUVmax) it exhibited an inverse correlation with tumor SUVmax. Tumor size on ^{18}F-FDG PET/CT showed a more linear correlation with pathology than that on MRI (r^2=0.91 vs 0.65). In Bland-Altman analysis, ^{18}F-FDG PET/CT showed significantly lower bias in size difference relative to pathology, compared with MRI (0.6±9.6cm vs. -1.9±17.3cm). Fluorine-18-FDG PET/CT showed more accurate T staging with pathology, especially in T3 cases, than MRI. **Conclusion:** A method of tumor size determination, using PHL on ^{18}F-FDG PET/CT, showed more linear relationship and smaller size differences with pathology than MRI (average 0.6 vs. 1.9cm). It provides sufficient reliability and reproducibility for measuring tumor size in breast cancer.

Hell J Nucl Med 2018; 21(2): 108-114 *Epub ahead of print: 12 July 2018* *Published online: 10 August 2018*

Introduction

Tumor size, which is a part of the TNM (tumor/nodes/metastases) staging system, is an important prognostic factor in patients with breast cancer. Accurate assessment of tumor size affects surgical strategy and prognosis prediction because post-surgical achievement of a negative resection margin can lower tumor recurrence [1, 2]. Breast-conservation therapy (BCT) is preferred in selected stage I and II breast cancer patients [3]. Many studies have demonstrated that BCT and mastectomy treatments yield similar prognoses in patients with stage I and II (up to 5cm in tumor size) breast cancer [4-6].

Preoperative tumor size can be measured using radiological imaging modalities: mammography (MG), ultrasonography (US) and magnetic resonance imaging (MRI). However, each of these modalities has limitations, such as the poor sensitivity of MG, high operator dependency of US, and high financial and labor cost of MRI. Among these, MRI exhibits the highest resolution and has been reported to most accurately estimate tumor size [7-9]. Although MRI showed high sensitivity (91% to 95%) and specificity (81% to 91%) in detecting breast cancer [10-12], there is a problem of overestimating tumor size in up to 56% of patients. Moreover, in tumors with T stages higher than T1, overestimation of size was reported in a higher proportion of patients (≤2cm: >2cm=18%: 49%) [13-17].

Positron emission tomography/computed tomography using 2-deoxy-2-fluoro-18-fluoro-D-glucose (^{18}F-FDG PET/CT) is a non-invasive method for evaluating glucose metabolism, and can serve as a useful modality for diagnosis, staging, restaging, and post-therapeutic response evaluation in breast cancer patients [18-21]. In detecting breast cancer, the sensitivity and specificity of ^{18}F-FDG PET/CT have been reported to be high, ranging from 80% to 96% and 83% to 100%, respectively [22-24]. However, the detection

rate was different according to tumor size (T1:T2=68%:91%) and concordance rate with pathologic T stage was relatively low (55%) [23, 24]. Generally, ^{18}F-FDG PET/CT has been considered inappropriate for evaluation of tumor size because of its poor spatial resolution, which limits clear delineation of the tumor boundary. Furthermore, ^{18}F-FDG PET/CT provides an inaccurate estimation of metabolic tumor volume (MTV), a known independent prognostic factor; thus, with using ^{18}F-FDG PET/CT it has been possible to obtain an approximate evaluation of the tumor volume only if based on fixed SUV threshold [25-27].

Recently, a volume measurement method using the peritumoral halo layer (PHL) has been proposed by Jun et al. (2015) for papillary thyroid cancer (PTC); this method relies on ^{18}F-FDG PET/CT [28]. This study was reported to be the most reliable when correlated with pathology, with smaller systemic divergent error and proportional error than estimates obtained by methods that use the fixed threshold (% SUVmax or SUV) on ^{18}F-FDG PET/CT. Although the PHL method appears promising for accurate estimation of tumor size and volume using ^{18}F-FDG PET/CT, it has not yet been fully validated. This study aimed to assess whether the PHL method, using ^{18}F-FDG PET/CT, is better than the MRI method and/or the usual ^{18}F-FDG PET/CT method for estimating tumor size in patients with breast cancer.

Patients and Methods

Patients

A total of 121 patients underwent ^{18}F-FDG PET/CT for clinical staging before initial treatment between March 2013 and May 2016. Patients were excluded if they had a history of neo-adjuvant treatment, preoperative mammotome, positive resection margin, ^{18}F-FDG non-avid tumor, clustered tumors, insufficient MRI (without contrast enhancement) or pathologic (such as absent size information) results. All enrolled 59 patients were treated with either BCT or simple/modified mastectomy. The following patient data were obtained from medical records: age, sex, MRI and/or ^{18}F-FDG PET/CT and/or surgery dates, surgery type, tumor location and pathologic type, and pathologic TNM (pTNM) stage (Table 1). The institutional review board approved the use of data from medical records for this retrospective study.

^{18}F-FDG PET/CT acquisition

Fluorine-18-FDG PET/CT was performed using two PET/CT scanners (DSTe 8; GE Medical Systems, Milwaukee, WI, USA, and Gemini 64; Philips Medical Systems, Andover, MA, USA). All patients fasted for ≥6 hours before scanning and serum glucose levels were checked prior to ^{18}F-FDG injection (DSTe: 0.2mCi/kg; Gemini: 0.1mCi/kg). Image acquisition began approximately 1 hour following ^{18}F-FDG injection. The scan range of ^{18}F-FDG PET/CT was from the base of the skull to the mid-thigh level. After low-dose CT scanning to correct for attenuation, PET acquisition began immediately in the same anatomical position (3-dimensional mode, 1.5-2.5min per bed position). Acquired images were reconstructed using an iterative ordered subsets expectation maximization algorithm, then transferred to a GE AW 4.5 workstation.

Image analysis: ^{18}F-FDG PET/CT and MRI

All ^{18}F-FDG PET/CT images were independently reviewed by two nuclear medicine physicians who were blinded to each patient's clinical information. When multifocal lesions were present in a patient, analysis was performed utilizing the largest tumor. The PHL in each tumor was determined using a previously published method [28]. First, an ^{18}F-FDG PET/CT image was modified using a 10-step color scale, based on the SUVmax of the tumor. Second, a color band that is representative of physiologic background activity was chosen. Third, using non-background color bands, the closest color band with irregularity that is different from the tumor shape was designated as the PHL. Fourth, the inner margin of the PHL was considered the tumor boundary. When the two reviewing physicians were in disagreement regarding the PHL of a particular image, a final decision was made via consultation with another nuclear medicine physician. Three-dimensional diameters [length (L), width (W) and height (H)] of the tumor on ^{18}F-FDG PET/CT were measured using the above-defined tumor margins. Three-dimensional diameters on MRI were measured in images of 2hr subtraction and sagittal MIP sequences. Tumor sizes on ^{18}F-FDG PET/CT and MRI were defined as the longest diameter among the 3-dimensional diameters. Figure 1 depicts the process used to define the tumor margin using a 10-step color scale on ^{18}F-FDG PET/CT.

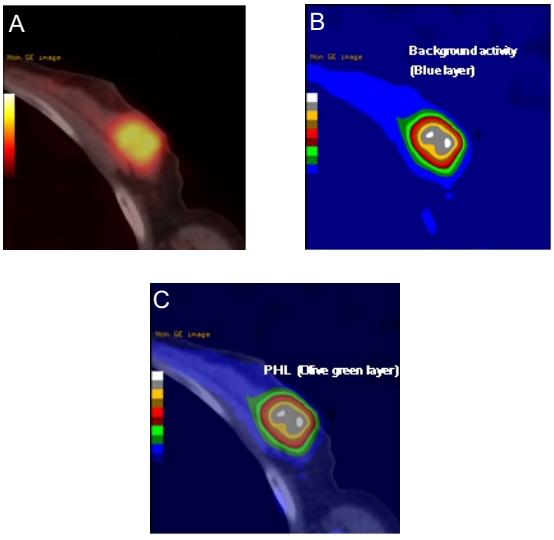

Figure 1. Example of PHL determination and measurement of tumor size on ^{18}F-FDG PET/CT. A. (PET/CT image), B. (PET image using 10-step color scale with SUV max adjustment), C. (fused PET/CT image using 10-step color scale). SUVmax of breast cancer is calculated by placing a spherical volume of interest over the tumor (A). The color map of PET is then changed to a 10-step color scale, which is calibrated by tumor SUVmax (dark blue layer=0-10% of tumor SUVmax, white layer=~90% of tumor SUVmax). Peri-tumoral halo layer (PHL) is defined as an abrupt increase in layer thickness, apart from background activity (physiologic breast uptake, blue color). In this example, PHL is the olive-green layer (20%-30% of tumor SUVmax) and the tumor boundary is the inner margin of the PHL (30% of tumor SUVmax) (B, C).

Pathologic tumor size as a standard reference

To calculate pathologic tumor size, three-dimensional diameters of each primary tumor (the largest tumor, in case of multifocal lesions) were obtained from pathology reports. Pathologic tumor size was determined as the longest diameter based on pathologic length, width, and height.

Statistical analysis

Statistical analysis was performed using MedCalc® 14.0 (MedCalc Software). Tumor sizes that were obtained from pathology, MRI and ^{18}F-FDG PET/CT were all described as mean± standard deviation (SD). Kappa statistics were used to evaluate the inter-observer agreement for determination of PHL surrounding each tumor. Correlations between pathology and MRI-determined tumor sizes, or between pathology and ^{18}F-FDG PET/CT-determined tumor sizes, were evaluated using linear regression analysis. Intraclass correlation coefficient (ICC) and Bland-Altman analyses were used to examine the concordance and reliability of tumor sizes obtained from MRI and ^{18}F-FDG PET/CT. P-values<0.05 were considered statistically significant.

Results

Patient characteristics

Fifty-nine patients with operable breast cancers were eligible for this study. Their characteristics are shown in Table 1. The mean time interval between ^{18}F-FDG PET/CT and surgery was 2 days (range, 0-15 days) and the mean SUVmax of the primary tumor was 5.2 (range, 1.4-15.4). The most common pathologic stage was pT2N0M0 (31%).

Table 1. *Characteristics of patients.*

Characteristics	All patients (n = 59)
Age, mean (range)	55 (41-89)
Sex (woman/man)	59/0
Surgery	
Breast-conservation therapy	33
Mastectomy	26
Pathologic type	
Ductal adenocarcinoma	52
Non-ductal adenocarcinoma	7
T stage, T1/T2/ T3	24/31/4
Tumor size (longest diameter), mm	
Pathology	26.4 (10.0-80.0)
MRI	28.3 (9.3-81.8)
PET/CT	25.8 (10.1-76.7)
SUVmax of tumor, mean (range)	5.2 (1.4-15.4)

Determination of PHL and inter-observer agreement

For the determination of PHL, inter-observer agreement between the two nuclear medicine physician reviewers was excellent (contingency coefficient=0.85, P<0.001). The PHL of each tumor was most commonly determined in the 20%-30% (olive-green color) band of SUVmax (27%). For the majority of the tumors (66%), PHL was detected in bands below the 40%-50% band. The distribution of PHL inversely correlated with the SUVmax of each tumor, as shown in Figure 2. Five discordant cases (8.5%) are shown in Table 2. With the exception of a single case, all discrepancies occurred in cases with relatively low levels of ^{18}F-FDG uptake (where SUVmax< 2.5), or in patients with small tumor sizes (T1). Figure 3 shows a representative case of breast cancer where the PHL band is of olive-green color (20%-30% of SUVmax).

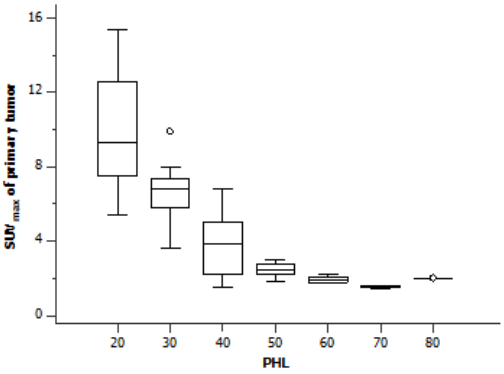

Figure 2. Relationship between SUVmax of primary tumor and PHL. Peri-tumoral halo layer (PHL) has a varied distribution and the %SUV of PHL tends to decrease as the SUVmax of the tumor increases. This indicates that the boundary of a high ^{18}F-FDG-avid tumor is wider than that of a low ^{18}F-FDG-avid tumor.

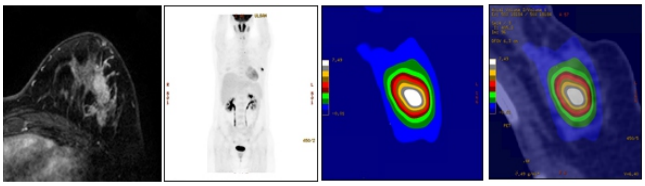

Figure 3. Representative case of a 34 years old patient with left breast cancer. Breast MRI (2min dynamic image) (A), Maximum intensity projection (MIP) image of ^{18}F-FDG PET/CT (B), trans-axial PET image using the 10-step color scale (C), trans-axial fused PET/CT image using the 10-step color scale (D). Pathologic tumor size was 25.0mm, while tumor size on MRI was 50.6mm (A). In PET/CT images, peri-tumoral halo layer (PHL) was designated as the olive-green color layer (20%-30% of SUVmax) and tumor margin was defined as the inner margin of PHL (white arrow) (C, D). The tumor size on PET was 20.7mm, which was substantially closer to the pathologic tumor size than the tumor size estimated by MRI.

Table 2. *Discordant assessment of PHL between the two physician reviewers.*

No	Age	Histologic type	SUVmax of tumor	Tumor size (LD), mm			PHL(%)	
				Pathology	MRI	PET/CT	Physician 1	Physician 2
1	65	Ductal	7.0	55.0	51.6	60.1	20	30
2	66	Ductal	1.9	14.0	13.7	14.0	60	50
3	49	Ductal	2.2	13.0	30.3	23.5	70	60
4	58	Ductal	2.0	15.0	41.1	12.4	70	80
5	52	Ductal	1.8	35.0	34.5	33.5	50	40

LD,longest diameter; PHL, peri-halolayer

Tumor sizes measured by ^{18}F-FDG PET/CT, MRI and pathology

Respective tumor sizes (mean±SD) on ^{18}F-FDG PET/CT, MRI and pathology measurements were 25.80±12.77mm, 28.32±12.97mm, and 26.27±14.35mm. Both MRI and PET/CT exhibited statistically significant correlations with pathology measurements in evaluation of tumor size. Fluorine-18-FDG PET/CT showed a more linear relationship with pathology measurements (r^2=0.91; P<0.0001) than did MRI (r^2=0.65, P<0.0001) (Figure 4). Differences in tumor size (mean±SD) on MRI and PET/CT, compared with pathology measurements, were 5.53±6.89mm and 3.34±3.00mm, respectively. In Bland-Altman analysis, the bias between ^{18}F-FDG PET/CT and pathology estimates was significantly smaller than the bias between MRI and pathology estimates (-1.9±17.3 vs. 0.6±9.6) (Figure 5). Intra-class correlation coefficient test demonstrated a higher concordance between ^{18}F-FDG PET/CT and pathology assessments of tumor size (0.95, 95% CI 0.91-0.97) than between MRI and pathology assessments of tumor size (0.80, 95% CI 0.69-0.88).

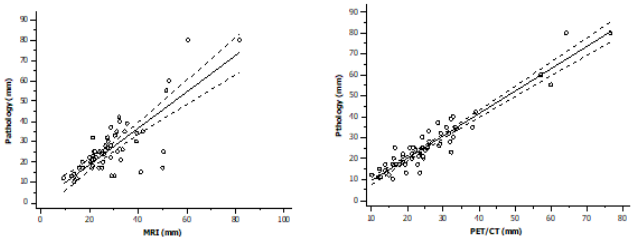

Figure 4. Linear regression analysis for tumor size: pathology vs. MRI and pathology vs. ^{18}F-FDG PET/CT. Although both ^{18}F-FDG PET/CT (right) and MRI (left) exhibited significant correlation with pathology in size measurement of tumor, ^{18}F-FDG PET/CT exhibited a more linear relationship than MRI (^{18}F-FDG PET/CT vs. MRI, r^2=0.91 vs. 0.65).

Correlation of ^{18}F-FDG PET/CT and MRI according to pathology T stage

There was a wide dispersion in tumor size between MRI and pathology, irrespective of T stage (T1 6.46±8.85, T2 4.60±5.10, T3 8.05±8.05). However, ^{18}F-FDG PET/CT exhibited a relatively lower variance in size difference for T1 and T2 stage tumors, compared with MRI (T1 2.70±2.63, T2 3.36±2.49, T3 6.70±6.09) (Figure 6). Table 3 displays the T stages and tumor sizes of 14 patients whose T stages were incorrect on MRI or ^{18}F-FDG PET/CT. Magnetic resonance imaging-assessed T stages were incorrect for 11 of 56 study patients (20%). All 11 cases were incorrectly upstaged on MRI (9 cases were upstaged T1 to T2; 1 case T1 to T3; 1 case T2 to T3). Fluorine-18-FDG PET/CT-assessed T stages were incorrect for seven patients. Four cases were upstaged (T1 to T2), while three cases were down-staged (T3 to T2). Among the mismatched 14 cases, four cases were incorrectly upstaged from T1 to T2 on both MRI and ^{18}F-FDG PET/CT.

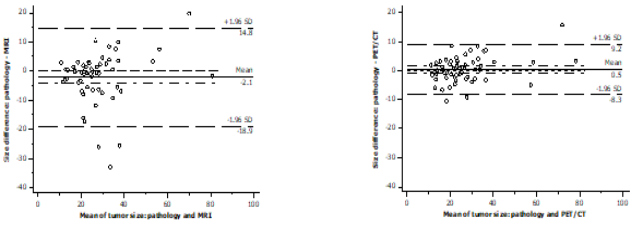

Figure 5. Bland-Altman plot for tumor sizes on pathology, MRI and ^{18}F-FDG PET/CT. ^{18}F-FDG PET/CT (right) shows a smaller difference in tumor size relative to pathology measurements, compared with MRI (left) (Bias, ^{18}F-FDG PET/CT vs. MRI=0.6±9.6 vs. -1.9±17.3).

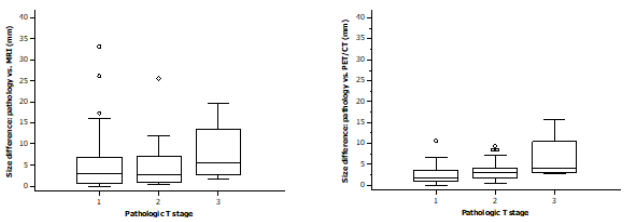

Figure 6. Size differences between pathology, MRI and ^{18}F-FDG PET/CT according to pathologic T stage. ^{18}F-FDG PET/CT (right) shows smaller size differences relative to pathology measurements compared with MRI (left), in all of T1, T2 and T3 stages.

Table 3. *Discordant estimates of pathologic Tstage, asassessed by ^{18}F-FDG PET/CT and MRI.*

No	T stage (measured tumor size, mm)			Size difference (mm)	
	Pathology	MRI	PET/CT	Pathology vs. MRI	Pathology vs. PET/CT
1	T1 (20.0)	T2 (25.6)	T2 (24.6)	5.6	4.6
2	T1	T2	T2	0.6	1.3
3	T2	T2	T1	0.9	2.2
4	T2	T3	T2	25.6	4.3
5	T1	T2	T2	17.3	10.5
6	T1	T2	T1	26.1	2.6
7	T1	T2	T2	4.0	5.9
8	T2	T2	T1	6.7	3.1
9	T1	T2	T1	3.4	0.8
10	T2	T2	T1	6.5	8.4
11	T1	T2	T1	6.9	2.5
12	T1	T2	T1	16.2	6.7
13	T1	T2	T1	8.1	0.8
14	T1	T3	T1	33.1	1.1

Discussion

To our knowledge, there has not yet been a clinical investigation of breast cancer tumor size estimates based on the ^{18}F-FDG PET/CT imaging modality. In this study, tumor size estimates obtained by a ^{18}F-FDG PET/CT method, which used PHL, demonstrated higher accuracy and correlation with pathologic tumor size than did tumor size estimates obtained by MRI.

Several past studies have demonstrated no difference in long-term survival between BCT and mastectomy in early breast cancer with tumors of relatively small size [3-6, 29]. Further, complete removal of the tumor reduces the chance of recurrence [1]. Thus, the ability to accurately evaluate tumor size and margin affects surgical strategy and may improve prognosis in breast cancer. Magnetic resonance imaging is often used to assess both tumor size and synchronous tumors because of its high-resolution and sensitivity [1]. However, several studies have reported that the published accuracy of tumor size measurement on MRI may be inaccurate [1, 13-15]. The concordance rate between MRI and pathologic tumor size was relatively low in a previous study (53%) [1]. Blair et al. (2006) demonstrated that the correlation of tumor size between MRI and pathology measurements is higher for high-grade tumors than for low-grade tumors [15]. Onesti et al. (2008) reported that significant size overestimation is present for breast tumors >2cm in size; thus, the sole use of MRI may increase the rate of unnecessary mastectomies [13].

The usefulness of ^{18}F-FDG PET/CT for staging breast cancer has been reported in many studies [24, 30-35]. However, these studies have focused on lymph node detection (N staging) or distant metastasis (M staging), while omitting tumor size (T stage). Moreover, several studies reported low concordance in T stage between pathology and ^{18}F-FDG PET/CT [23, 24]. An unclear tumor margin on ^{18}F-FDG PET/CT, arising from its inherently low resolution and from the confounding factor of surrounding physiologic breast uptake, is likely the main reason that PET/CT is not used for tumor size evaluation. Recently, there have been reports that MTV is a valid independent prognostic factor to predict survival in patients with breast cancer [26, 36, 37]. Metabolic tumor volume is typically calculated by %SUVmax (MTV% SUVmax) or by SUV threshold methods. However, MTV measured by these methods underestimate the tumor burden

because these methods do not include all ^{18}F-FDG-avid portions of the tumor. Accurate measurement of the metabolically active tumor burden requires accurate delineation of the tumor margin. Recently, a method using PHL has been reported as reliable in measuring tumor volume in cases of thyroid cancer [28]. These reports suggest that PHL can enhance tumor margin detection on ^{18}F-FDG PET/CT.

Following the method of the previous study, we used a color band to group the continuous reduction of tumor ^{18}F-FDG uptake (from the center of the tumor to its border) into 10% reduction scales. Peri-tumoral halo layer is defined as the band where the width changes most suddenly amongst the 10 bands; tumor margin on ^{18}F-FDG PET/CT is thus defined as the inner margin of PHL. This method is similar in theory to the gradient-based method for determining tumor margins using specialized software; however, the PHL method is more intuitive and straightforward [38]. Notably, inverse correlations between SUVmax and tumor boundary have been reported in previous studies [28, 39]; in this study, PHL in breast cancer was also inversely correlated with tumor SUVmax, which suggests that the PHL method is quite similar to the gradient-based method for evaluation of tumor size.

The determination of PHL in breast cancer was consistent between two independent nuclear medicine experts in this study. Four of nine (44%) lesions with low ^{18}F-FDG-avid exhibited discordant results when evaluated by PHL. High normal breast activity surrounding the tumor may interfere with determination of PHL in low ^{18}F-FDG-avid lesions. Small -sized tumors exhibited a tighter distribution of color bands than did large-sized tumors, increasing the difficultly in determining PHL. The determination of PHL in breast cancer should focus on a clear distinction between normal breast activity and tumor ^{18}F-FDG uptake; importantly, heterogeneous ^{18}F-FDG uptake related to central necrosis should be taken into consideration. Therefore, a centripetal method may be more effective in determining PHL than the centrifugal method that was used in the previous study of thyroid cancer.

The longest tumor diameters exhibited statistically smaller differences and more linear correlations between ^{18}F-FDG PET/CT and pathology, compared with MRI and pathology. This demonstrates that ^{18}F-FDG PET/CT can provide accurate tumor size estimates, which can aid in determining an appropriate surgical strategy and in prognostic prediction. Magnetic resonance imaging assessment indicated inaccurate T stages in 20% of the patients in this study; in contrast, ^{18}F-FDG PET/CT indicated inaccurate T stages in only 13% of the patients. Further, MRI assessments resulted in two patients incorrectly upstaged as T3; ^{18}F-FDG PET/CT assessments avoided this error. Estimated size differences in 14 incorrectly staged patients were also smaller on ^{18}F-FDG PET/CT assessment than on MRI assessment. Overestimation of tumor size on MRI may needlessly deprive a patient of the opportunity for BCT, which is a simpler and more superficial therapy than mastectomy. Thus, tumor size estimates using ^{18}F-FDG PET/CT may be more reliable in guiding surgical strategy for large-sized tumors.

Accurate assessment of tumor size includes accurate assessment of tumor volume. However, we have discussed the challenges of MTV using a fixed % SUVmax (MTV%SUVmax) threshold, such as 50% SUVmax, which may underestimate MTV compared to PTV; consequently, there has been discussion of the need for a suitable SUV threshold for each type of tumor, rather than a generalized fixed threshold [40, 41]. In our study, tumor margins were commonly determined at <50% of SUVmax, which may further support the call for individualized SUV thresholds. The relationship between PHL and the SUVmax of the tumor, as determined in this study, reinforces this stance. The PHL-based study of thyroid cancer revealed that when a flexible SUV threshold (MTV-PHL) was used, correlations between PTV and the SUV threshold were higher than correlations between PTV and a fixed threshold, MTV%SUVmax. However, unlike thyroid cancer, breast cancer often exhibits a larger, irregular shape; thus, it may exhibit different results from thyroid cancer. Further investigation is needed to determine the relationship between MTVPHL and PTV, as well as their usefulness in predicting the prognosis of patients with breast cancer.

There are several limitations in this study. Importantly, this was performed in a single institution and may therefore lack representation or suffer from selection bias. However, this may not seriously affect the results because the purpose of this study was simply to evaluate and compare the reliability of a tumor size measurement method using PHL; moreover, the included cases exhibited various tumor sizes. Pathologic size that was used as a reference standard was solely acquired through review of pathologic reports; there may be changes in pathologic measurement during preservation and preparation of each tissue specimen. Time intervals may also contribute to the differences in measured values.

In conclusion, the method of using PHL on ^{18}F-FDG PET/CT accurately assessed pathologic tumor size in breast cancer. Although this method may overestimate small lesions, it exhibited greater correlation and reliability with pathology measurements (compared with MRI) and accurately assessed T3 tumors.

Bibliography

1. Grimsby GM, Gray R, Dueck A et al. Is there concordance of invasive breast cancer pathologic tumor size with magnetic resonance imaging? *Am J Surg* 2009; 198: 500-4.
2. Amano G, Ohuchi N, Ishibashi T et al. Correlation of three-dimensional magnetic resonance imaging with precise histopathological map concerning carcinoma extension in the breast. *Breast Cancer Res Treat* 2000; 60: 43-55.
3. Fisher B, Anderson S, Bryant J et al. Twenty-year follow-up of a randomized trial comparing total mastectomy, lumpectomy, and lumpectomy plus irradiation for the treatment of invasive breast cancer. *N Engl J Med* 2002; 347: 1233-41.
4. Poggi MM, Danforth DN, Sciuto LC et al. Eighteen-year results in the treatment of early breast carcinoma with mastectomy versus breast conservation therapy: the National Cancer Institute Randomized Trial. *Cancer* 2003; 98: 697-702.
5. Jacobson JA, Danforth DN, Cowan KH et al. Ten-year results of a comparison of conservation with mastectomy in the treatment of stage I and II breast cancer. *N Engl J Med* 1995; 332: 907-11.
6. Arriagada R, Le MG, Rochard F, Contesso G. Conservative treatment versus mastectomy in early breast cancer: patterns of failure with 15 years of follow-up data. Institut Gustave-Roussy Breast Cancer Group.

J Clin Oncol 1996; 14: 1558-64.
7. Hata T, Takahashi H, Watanabe K et al. Magnetic resonance imaging for preoperative evaluation of breast cancer: a comparative study with mammography and ultrasonography. *J Am Coll Surg* 2004; 198: 190-7.
8. Boetes C, Veltman J, van Die L et al. The role of MRI in invasive lobular carcinoma. *Breast Cancer Res Treat* 2004; 86: 31-7.
9. Weatherall PT, Evans GF, Metzger GJ et al. MRI vs. histologic measurement of breast cancer following chemotherapy: comparison with x-ray mammography and palpation. *J Magn Reson Imaging* 2001; 13: 868-75.
10. Law Y, Cheung PS, Lau S, Lo GG. Impact of magnetic resonance imaging on preoperative planning for breast cancer surgery. *Hong Kong Med J* 2013; 19: 294-9.
11. Lo GG, Ai V, Chan JK et al. Diffusion-weighted magnetic resonance imaging of breast lesions: first experiences at 3 T. *J Comput Assist Tomogr* 2009; 33: 63-9.
12. Kuhl CK, Schrading S, Leutner CC et al. Mammography, breast ultrasound and magnetic resonance imaging for surveillance of women at high familial risk for breast cancer. *J Clin Oncol* 2005; 23: 8469-76.
13. Onesti JK, Mangus BE, Helmer SD, Osland JS. Breast cancer tumor size: correlation between magnetic resonance imaging and pathology measurements. *Am J Surg* 2008; 196: 844-8; discussion 9-50.
14. Orel SG, Schnall MD. MR imaging of the breast for the detection, diagnosis, and staging of breast cancer. *Radiol* 2001; 220: 13-30.
15. Blair S, McElroy M, Middleton MS et al. The efficacy of breast MRI in predicting breast conservation therapy. *J Surg Oncol* 2006; 94: 220-5.
16. Haraldsdottir KH, Jonsson T, Halldorsdottir AB et al. Tumor size of invasive breast cancer on magnetic resonance imaging and conventional imaging (Mammogram/Ultrasound): comparison with pathological size and clinical implications. *Scand J Surg* 2017; 106: 68-73.
17. Lai HW, Chen DR, Wu YC et al. Comparison of the diagnostic accuracy of magnetic resonance imaging with sonography in the prediction of breast cancer tumor size: A concordance analysis with histopathologically determined tumor size. *Ann Surg Oncol* 2015; 22: 3816-23.
18. Robertson IJ, Hand F, Kell MR. FDG-PET/CT in the staging of local/regional metastases in breast cancer. *Breast* 2011; 20: 491-4.
19. Uematsu T, Kasami M, Yuen S. Comparison of FDG PET and MRI for evaluating the tumor extent of breast cancer and the impact of FDG PET on the systemic staging and prognosis of patients who are candidates for breast-conserving therapy. *Breast Cancer* 2009; 16: 97-104.
20. Cermik TF, Mavi A, Basu S, Alavi A. Impact of FDG PET on the preoperative staging of newly diagnosed breast cancer. *Eur J Nucl Med Mol Imaging* 2008; 35: 475-83.
21. Zhang X, Wu F, Han P. The role of ^{18}F-FDG PET/CT in the diagnosis of breast cancer and lymph nodes metastases and micrometastases may be limited. *Hell J Nucl Med* 2014; 17: 177-83.
22. Lim HS, Yoon W, Chung TW, et al. FDG PET/CT for the detection and evaluation of breast diseases: usefulness and limitations. *Radiographics* 2007; 27 Suppl 1: S197-213.
23. Avril N, Rose CA, Schelling M et al. Breast imaging with positron emission tomography and fluorine-18 fluorodeoxyglucose: use and limitations. *J Clin Oncol* 2000; 18: 3495-502.
24. Riegger C, Herrmann J, Nagarajah J et al. Whole-body FDG PET/CT is more accurate than conventional imaging for staging primary breast cancer patients. *Eur J Nucl Med Mol Imag* 2012; 39: 852-63.
25. Jimenez-Ballve A, Garcia Garcia-Esquinas M, Salsidua-Arroyo O et al. Prognostic value of metabolic tumour volume and total lesion glycolysis in ^{18}F-FDG PET/CT scans in locally advanced breast cancer staging. *Rev Esp Med Nucl Imagen Mol* 2016; 35: 365-72.
26. Son SH, Lee SW, Jeong SY et al. Whole-Body Metabolic Tumor Volume, as Determined by ^{18}F-FDG PET/CT, as a Prognostic Factor of Outcome for Patients With Breast Cancer Who Have Distant Metastasis. *Am J Roentgenol* 2015; 205: 878-85.
27. Marinelli B, Espinet-Col C, Ulaner GA et al. Prognostic value of FDG PET/CT-based metabolic tumor volumes in metastatic triple negative breast cancer patients. *Am J Nucl Med Mol Imag* 2016; 6: 120-7.
28. Jun S, Kim H, Nam HY. A new method for segmentation of FDG PET metabolic tumour volume using the peritumoural halo layer and a 10-step colour scale. A study in patients with papillary thyroid carcinoma. *Nuklearmedizin* 2015; 54: 272-85.
29. Veronesi U, Cascinelli N, Mariani L et al. Twenty-year follow-up of a randomized study comparing breast-conserving surgery with radical mastectomy for early breast cancer. *N Engl J Med* 2002; 347: 1227-32.
30. Pritchard KI, Julian JA, Holloway CM et al. Prospective study of 2-[^{18}F]fluorodeoxyglucose positron emission tomography in the assessment of regional nodal spread of disease in patients with breast cancer: an Ontario clinical oncology group study. *J Clin Oncol* 2012; 30: 1274-9.
31. Caresia Aroztegui AP, Garcia Vicente AM, Alvarez Ruiz S et al. ^{18}F-FDG PET/CT in breast cancer: Evidence-based recommendations in initial staging. *Tumour Biol* 2017; 39: 1010428317728285.
32. Ulaner GA, Castillo R, Wills J et al. ^{18}F-FDG-PET/CT for systemic staging of patients with newly diagnosed ER-positive and HER2-positive breast cancer. *Eur J Nucl Med Mol Imaging* 2017; 44: 1420-7.
33. Hogan MP, Goldman DA, Dashevsky B et al. Comparison of ^{18}F-FDG PET/CT for Systemic Staging of Newly Diagnosed Invasive Lobular Carcinoma Versus Invasive Ductal Carcinoma. *J Nucl Med* 2015; 56: 1674-80.
34. Ulaner GA, Castillo R, Goldman DA et al. ^{18}F-FDG-PET/CT for systemic staging of newly diagnosed triple-negative breast cancer. *Eur J Nucl Med Mol Imag* 2016; 43: 1937-44.
35. Kong EJ, Chun KA, Bom HS et al. Initial experience of integrated PET/MR mammography in patients with invasive ductal carcinoma. *Hell J Nucl Med* 2014; 17: 171-6.
36. Kim J, Yoo SW, Kang SR et al. Prognostic Significance of Metabolic Tumor Volume Measured by ^{18}F-FDG PET/CT in Operable Primary Breast Cancer. *Nucl Med Mol Imag* 2012; 46: 278-85.
37. Hyun SH, Ahn HK, Park YH et al. Volume-based metabolic tumor response to neoadjuvant chemotherapy is associated with an increased risk of recurrence in breast cancer. *Radiol* 2015; 275: 235-44.
38. Werner-Wasik M, Nelson AD, Choi W et al. What is the best way to contour lung tumors on PET scans? Multiobserver validation of a gradient-based method using a NSCLC digital PET phantom. *Int J Radiat Oncol Biol Phys* 2012; 82: 1164-71.
39. Hyun SH, Choi JY, Shim YM et al. Prognostic value of metabolic tumor volume measured by 18F-fluorodeoxyglucose positron emission tomography in patients with esophageal carcinoma. *Ann Surg Oncol* 2010; 17: 115-22.
40. Yu J, Li X, Xing L et al. Comparison of tumor volumes as determined by pathologic examination and FDG-PET/CT images of non-small-cell lung cancer: a pilot study. *Int J Radiat Oncol Biol Phys* 2009; 75: 1468-74.
41. Sridhar P, Mercier G, Tan J et al. FDG PET metabolic tumor volume segmentation and pathologic volume of primary human solid tumors. *Am J Roentgenol* 2014; 202: 1114-9.